Asian Journal of Chemistry; Vol. 25, No. 16 (2013), 9055-9058

ASIAN JOURNAL OF CHEMISTRY

http://dx.doi.org/10.14233/ajchem.2013.14985

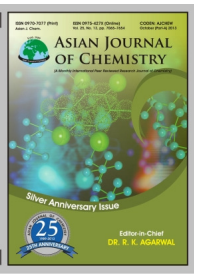

Effects of Surfactants on the Microstructure Characteristics of Alumina Microfibers

PENG WANG[1,*], ZHENDONG ZHAO[2], ZONGDE WANG[1], MIN HUANG[1], SHANGXING CHEN[1] and GUORONG FAN[1]

[1]College of Forest, Jiangxi Agriculture University, Nanchang 330045, P.R. China
[2]Institute of Chemical Industry of Forest Products, CAF; National Engineering Lab. for Biomass Chemical Utilization; Key and Open Lab. on Forest Chemical Engineering, SFA, Nanjing 210042, P.R. China

*Corresponding author: Tel: +86 791 83828029; E-mail: pengwang1981@126.com

(*Received*: 15 December 2012; *Accepted*: 16 September 2013) AJC-14112

Alumina microfibers were synthesized using different types of surfactants (rosin-based quaternary ammonium salt, sodium dodecyl sulphate and triblock copolymer P123 as directing agents. Their structures were characterized with X-ray diffraction, N_2 adsorption and desorption, field-emission scanning electron microscope and transmission electron microscopy to investigate the effects of surfactants on the microstructure characteristics of alumina microfibers. The surfactants can not change the intrinsic crystal structure of the as-syntheiszed ammonium aluminium carbonate hydroxide with the composition ($NH_4[Al(OH)_2CO_3]$) (AACH), but they will alter the way of the growth of the AACH nanocrystals. Because of the strong electrostatic interaction between AACH nanocrystals and ionic surfactants (rosin-based quaternary ammonium salt and sodium dodecyl sulphate), the AACH microfibers grew too fast on the surfactant micelles to form regular fibrous morphologies. When the non-ionic surfactant P123 was used as the template, due to the weak hydrogen bond interaction, the AACH microfibers grew at an appropriate speed to form a uniform fibrous morphology.

Key Words: Alumina microfiber, Morphology, Surfactant, Rosin-based quaternary ammonium salt.

INTRODUCTION

Because of the rich porosities and large surface areas as well as the outstanding thermal and mechanical stabilities, mesoporous alumina are widely used in the areas of catalysis, separation and adsorption[1-3]. However, the preformances of mesoporous alumina depend not only on their porosities and surface areas, but also on their morphologies. Special morphologies often bring mesoporous alumina with varieties of physical and chemical properties, such as high dielectric constant, large mechanical modulus, *etc*.[4,5].

Surfactants play a crucial role in the morphology modification process of mesoporous aluminas. Several researchers have demonstrated the synthesis of mesoporous alumina with various shapes using different kinds of surfactants. Su *et al*.[6] demonstrated the synthesis of lamellate structure mesoporous alumina with the assistance of non-ionic surfactant PEG6000 using $Al_2(SO_4)_3$ and $NaAlO_2$ as aluminum precursors. Bai *et al*.[7] prepared mesoporous alumina microfibers under hydrothermal conditions using tri-block copolymer P123 as directing agent and urea as homogeneous precipitation agent. Through the same method, multilayered alumina microfibers and alumina nanorods were successfully synthesized by Zhu *et al*.[8-10] using different kinds of PEG (polyethylene glycol) as directing agents. Mesoporous aluminas with spheres, rods, fibers and three-dimensional dumbbells, flower-like hierarchical superstructures were obtained by Liu *et al*.[11] using cetyltrimethylammonium bromide and sodium dodecyl sulphate as directing agents.

We have developed a facile and economic ammonium carbonate precipitation method for preparing mesoporous alumina microfibers in our previous work[12]. In the present work, different types of surfactants (cationic, anionic and non-ionic surfactants) were introduced in the process of ammonium carbonate precipitation method for the synthesis of alumina microfibers. The influences of the surfactants on the microstructure characteristics of the materials were investigated.

EXPERIMENTAL

Rosin-based quaternary ammonium salt[13] [(RSAC), technical grade, principal component: abietyltrimethyl ammonium chloride] was provided by Henan Titaning Chemical Technology Co., Ltd. Sodium dodecyl sulphate (SDS, AR) was purchased from Chengdu Kelong Reagent Chemical Factory. Triblock copolymer $(PEO)_{20}$-$(PPO)_{70}$-$(PEO)_{20}$, namely P123, was provided by Sigma-Aldrich Co. Aluminium nitrate nonahydrate (AR) was purchased from Shanghai Zhenxin Reagent Chemical Factory. Ammonium carbonate (AR) was provided by Guangdong Chemical Reagent Engineering-Technological Research and Development Center.

General procedure: In a typical experiment, three kinds of surfactants (RSAC, SDS and P123) were dissolved in 50 mL 0.5 mol/L aluminium nitrate solution at 343 K, respectively. The molar ratio of aluminium nitrate to sufactants was 1:0.02. 150 mL of 0.5 mol/L ammonium carbonate solution was then added while stirred. After stirring for 2 h, the precipitate was aged at 343 K for 18 h and washed with water and ethanol for several times. After drying at 323 K, the template agents were removed by calcination at 833 K for 4 h at the rate of 1 K/min. The results were denoted as A-RSAC, A-SDS and A-P123.

Detection method: The crystalline phases of the samples were recorded by an X-ray diffractometer (D8 Focus, Bucker AXS Inc., Germany) with CuK_α radiation (k = 0.154 nm). The operating target voltage was 40 kV and the current was 40 mA. The sample was powdered and scanned for 2θ ranging from 10-80º. Porosity and surface area measurements were performed following the N_2 adsorption on a Micromeritics ASAP2020 instrument made by Micromeritics Instrument Corporation. The special surface areas were calculated using the Brunauer-Emmett-Teller (BET) model. Average pore diameters were calculated using the Barrett-Joyner-Halenda (BJH) method from the desorption branch of isotherm. The microscopic features of the samples were characterized with a field-emission scanning electron microscope (S-4800 HITACHI, Japan) operated at 5 KV. Transmission electron microscopy images were obtained with a JEOL JEM-2100 instrument operated at an accelerating voltage of 200 kV. The samples were ultrasonically dispersed in ethanol and then dropped onto the carbon-coated copper grids prior to the measurements.

RESULTS AND DISCUSSION

Fig. 1 shows the XRD patterns of the as-synthesized alumina microfibers. All the peaks of the samples can be indexed to the data available in the JCPDS 42-0250 powder diffraction file, indicating that all the samples contain only a AACH ($NH_4[Al(OH)_2CO_3]$) crystalline phase. No distinct dissimilarity can be observed from the patterns of the as-synthesized samples, suggesting that surfactants can not change the intrinsic crystal structure of AACH. This result is similar to Zhu *et al.*[14] report.

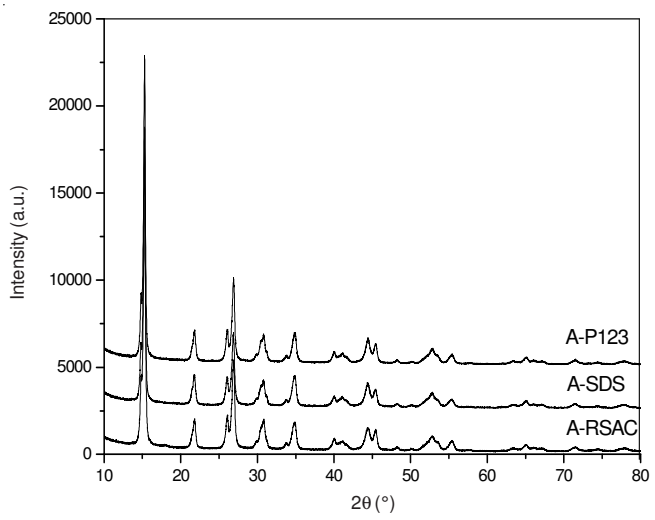

Fig. 1. XRD patterns of the as-synthesized alumina microfibers

XRD patterns of calcined samples are shown in Fig. 2. The sample of A-RSAC displays diffraction lines of the γ-Al_2O_3 phase (JCPDS card No. 10-425). The other two samples only exhibit two broad humps, implying the existence of amorphous aluminas. Although the surfactants can not change the intrinsic crystal structure of precursor, but they have a great impact on crystalline structure of the samples after calcination. The season for this phenomenon can be related to the residue of the Cl^- ion from RSAC in calcination.

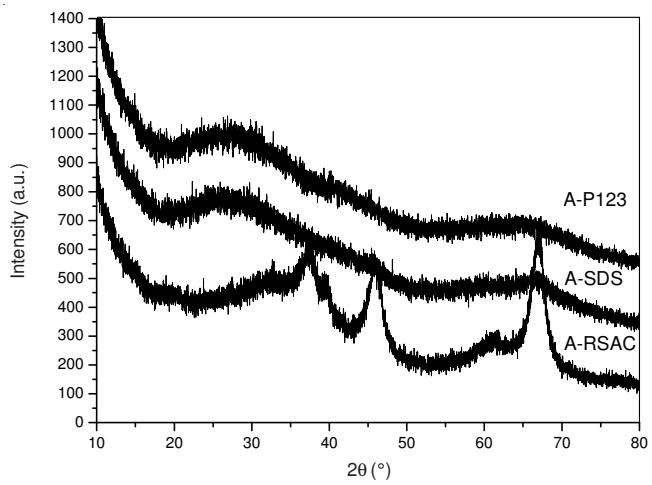

Fig. 2. XRD patterns of calcined alumina microfibers

Fig. 3 shows the N_2 adsorption-desorption isotherms of the calcined alumina microfibers. All the samples exhibit classical type IV isotherm (classification by IUPAC) which is a characteristic of mesoporous material. The hysteresis loops of the samples are different, indicating that there are great differences in pore structures of the samples. BJH pore size distributions of the samples are depicted in Fig. 4. The curve of the A-RSAC sample displays a bimodal pattern. The pores with the smaller sizes bear concentrate distribution at 3.8 nm, while those with the larger sizes possess broad distribution in the range of 5.5-14 nm. The curves of the samples A-SDS and A-P123 exhibit a single peak distribution centered at 3.8 nm. Table-1 summarizes the textural properties of the three samples. It can be noted that all the samples possess big specific surface areas. The sample A-SDS shows the biggest specific surface area (369.45 m^2/g), the highest pore volume (0.62 cm^3/g) and the largest pore diameter (5.74 nm).

Fig. 5 shows the field-emission SEM images of as-synthesized and calcined samples. All the as-synthesized samples reveal a fibrous morphology (Fig. 5a-e) due to the formation of AACH. However, significant differences can also be observed among the samples. The as-synthesized microfibers directed by RSAC are various in sizes and wider than the other two samples (Fig. 5a), while the ones synthesized by SDS are shorter with an obvious sense of fragmentation (Fig. 5c). Well dispersed and uniform microfibers can be observed in the image (Fig. 5e) of the sample templated by P123. Thus, the surfactants have great effects on the morphologies of the samples. Although the surfactants can not change the intrinsic crystal structure of AACH, but they will alter the way of the growth of the AACH nanocrystals. Different types of surfactants

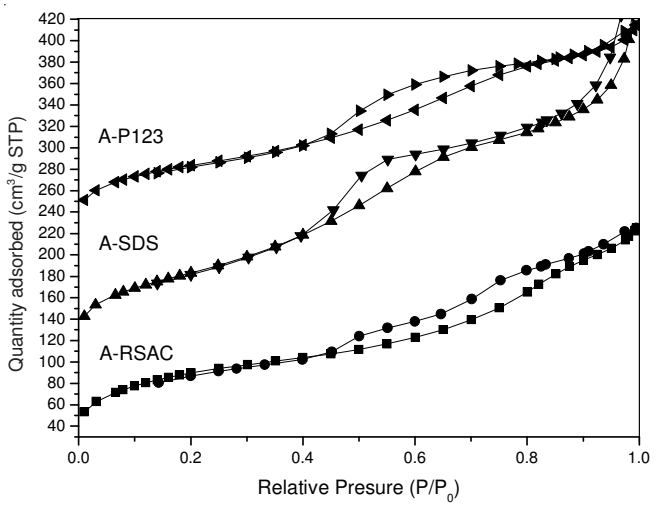

Fig. 3. N_2 adsorption-desorption isotherms of calcined alumina microfibers

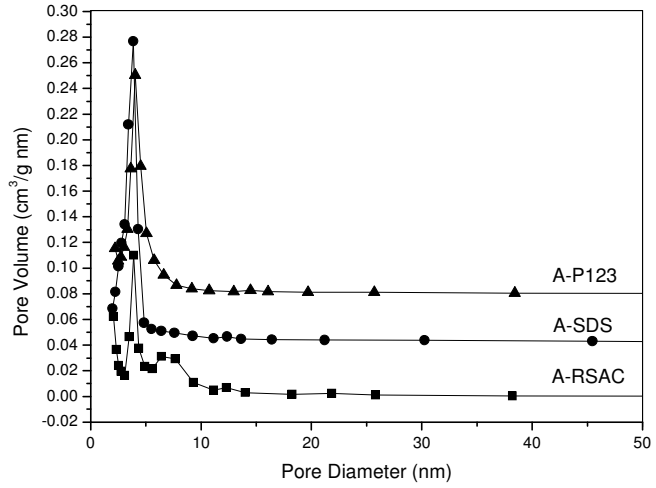

Fig. 4. BJH pore size distributions of calcined alumina microfibers

TABLE-1
TEXTURAL PROPERTIES OF
CALCINED ALUMINA MICROFIBERS

Sample	S_{BET} (m^2/g)	V (cm^3/g)	D (nm)
A-RSAC	323.45	0.33	5.32
A-SDS	369.45	0.62	5.74
A-P123	298.75	0.36	4.85

possess various charging properties. When the surfactants of RSAC and SDS were applied as the directing agents, the as-synthesized AACH nanocrystals were bonded to the surfactant micelles through the electrostatic interaction in order to form fibrous structures. However, due to this strong interaction, the AACH microfibers grew so fast that the irregularly fibrous morphologies were formed. When the surfactant P123 was used as the template, the AACH nanocrystals and the surfactant micelles was interacted with hydrogen bond which was weaker than the electrostatic interaction. Thus, the AACH microfibers grew at an appropriate speed to form a uniform fibrous morphology. It can be seen that the morphology of the alumina samples was not markedly altered after the calcination at 833 K for 4 h (Fig. 5b-f).

For further investigation of the morphology and microstructures of the calcined alumina microfibers, transmission

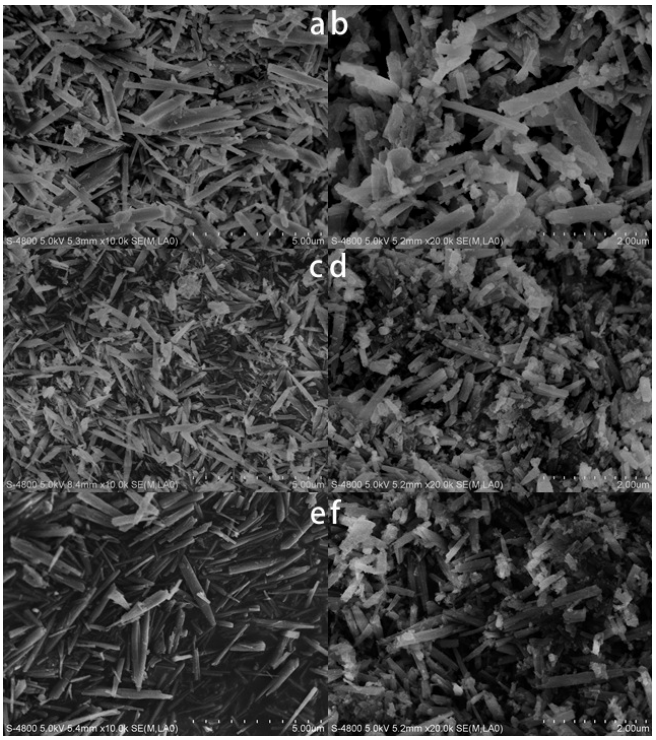

Fig. 5. Field emission SEM images of as-synthesized (a, c, e) and calcined (b, d, f) alumina microfibers; a, b: A-RSAC; c,d: A-SDS; e,f: A-P123

electron microscopy was applied. All the calcined samples display a fibrous morphology with wormhole-like mesopores (Fig. 6). It can be seen that the edges of the A-RSAC sample are rough (Fig. 6a-b), while the A-SDS sample shows obvious fracture phenomenon of the microfibers (Fig. 6c-d). Only the A-P123 sample is made of integrated microfibers with smooth edges (Fig. 6e-f). The results are in good agreement with the field emission SEM characterizations.

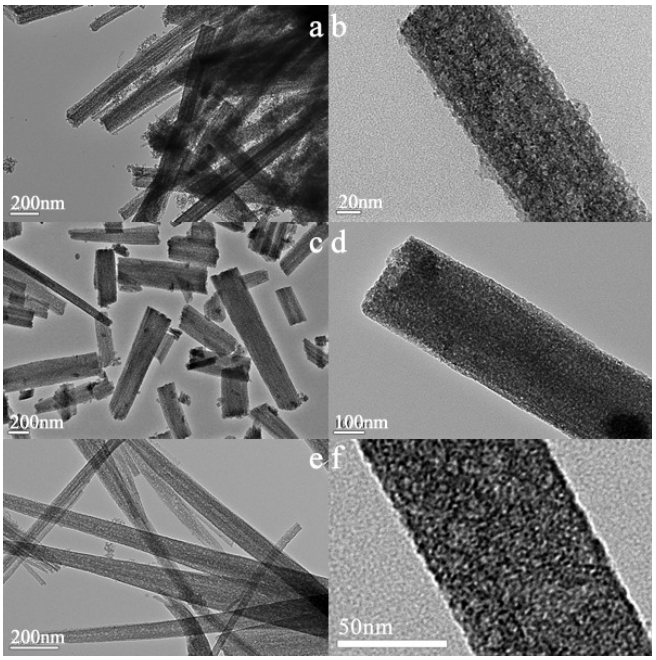

Fig. 6. TEM images of calcined alumina microfibers; a, b: A-RSAC; c,d: A-SDS; e,f: A-P123

Conclusion

Different types of surfactants (RSAC, SDS and P123) were introduced in the process of the synthesis of alumina microfibers. The effects of surfactants on the microstructure characteristics of alumina microfibers were investigated. The surfactants can not change the intrinsic crystal structure of the as-syntheiszed AACH, but they will alter the way of the growth of the AACH nanocrystals. Because of the strong electrostatic interaction between AACH nanocrystals and ionic surfactants (RSAC, SDS), the AACH microfibers grew too fast on the surfactant micelles to form regular fibrous morphologies. When the surfactant P123 was used as the template, due to the weak hydrogen bond interaction, the AACH microfibers grew at an appropriate speed to form a uniform fibrous morphology.

ACKNOWLEDGEMENTS

This work was supported by the Jiangxi Agriculture University Starting Foundation for Doctoral Research (grant No. 09004314), the Natural Science Foundation of China (grant No. 30972319) and the Joint Innovation of Industries, Universities and Research Institutes Foundation (grant No. BY2010112).

REFERENCES

1. M.E. Doukkali, A. Iriondo, P.L. Arias, J. Requies, I. Gandarías, L. Jalowiecki-Duhamel and F. Dumeignil, *Appl. Catal. B*, **125**, 516 (2012).
2. C. Chen and W.-S. Ahn, *Chem. Eng. J*., **166**, 646 (2011).
3. B. Yahyaei and S. Azizian, *Chem. Eng. J*., **209**, 589 (2012).
4. J. Zou, L. Pu, X. Bao and D. Feng, *Appl. Phys. Lett*., **80**, 1079 (2002).
5. X.S. Fang, C.H. Ye, L.D. Zhang and T. Xie, *Adv. Mater*., **17**, 1661 (2005).
6. A. Su, Y. Zhou, Y. Yao, C. Yang and H. Du, *Micropor. Mesopor. Mater*., **36**, 159 (2012).
7. P. Bai, F. Su, P. Wu, L. Wang, F.Y. Lee, L. Lv, Z.F. Yan and X.S. Zhao, *Langmuir*, **23**, 4599 (2007).
8. Z. Zhu, H. Sun, H. Liu and D. Yang, *J. Mater. Sci*., **45**, 46 (2010).
9. Z. Zhu, H. Liu, H. Sun and D. Yang, *Chem. Eng. J*., **155**, 925 (2009).
10. Z. Zhu, H. Liu, H. Sun and D. Yang, *Micropor. Mesopor. Mater*., **123**, 39 (2009).
11. Q. Liu, A. Wang, X. Wang and T. Zhang, *Micropor. Mesopor. Mater*., **100**, 35 (2007).
12. P. Wang, Z.D. Zhao, L.W. Bi, Y.X. Chen, L. Zhang and L.T. Sun, *Mater. Res. Innov*., **16**, 121 (2012).
13. P. Wang, Z.D. Zhao, L.W. Bi and Y.X. Chen, *Asian J. Chem*., **24**, 3439 (2012).
14. H.Y. Zhu, J.D. Riches and J.C. Barry, *Chem. Mater*., **14**, 2086 (2002).